

Josephson effect in graphene SBS junctions

Maitri Maiti and K. Sengupta

TCMP division, Saha Institute of Nuclear Physics, 1/AF Bidhannagar, Kolkata-700064, India.

(Dated: March 23, 2024)

We study Josephson effect in graphene superconductor-barrier-superconductor junctions with short and wide barriers of thickness d and width L , which can be created by applying a gate voltage V_0 across the barrier region. We show that Josephson current in such graphene junctions, in complete contrast to their conventional counterparts, is an oscillatory function of both the barrier width d and the applied gate voltage V_0 . We also demonstrate that in the thin barrier limit, where $V_0 \ll 1$ and $d \ll 0$ keeping $V_0 d$ finite, such an oscillatory behavior can be understood in terms of transmission resonance of Dirac-Bogoliubov-de Gennes quasiparticles in superconducting graphene. We discuss experimental relevance of our work.

PACS numbers: 74.50+r, 74.45.+c, 74.78.Na

I. INTRODUCTION

Graphene, a two-dimensional single layer of graphite, has been recently fabricated by Novoselov et al.¹. In graphene, the energy bands touch the Fermi energy at six discrete points at the edges of the hexagonal Brillouin zone. Two of these six Fermi points, referred to as K and K^0 points, are inequivalent and the quasiparticle excitations about them obey linear Dirac-like energy dispersion². The presence of such Dirac-like quasiparticles leads to a number of unusual electronic properties in graphene including relativistic quantum hall effect with unusual structure of Hall plateaus³, which has been verified in experiments⁴. Further, as suggested in Ref. 5, Dirac quasiparticles in graphene leads to realization of interesting physical phenomenon such as Klein paradox^{4,6}, Lorenz-boost type phenomenon⁷, and unconventional Kondo effect^{8,9}.

Another interesting consequences of the existence of Dirac-like quasiparticles can be understood by studying superconductivity in graphene. It has been suggested that superconductivity can be induced in a graphene layer in the presence of a superconducting electrode near it via proximity effect^{10,11,12} or by intercalating it with metallic atoms¹³. Consequently, studies on tunneling conductance on both normal metal-superconductors (NS) and normal metal-barrier-superconductor (NBS) junctions in graphene have been undertaken^{10,14,15}. It has been shown in Refs. 14 and 15 that the tunneling conductance of such NBS junctions are oscillatory functions of the effective barrier strength and that this oscillatory phenomenon can be understood in terms of transmission resonance phenomenon of Dirac-Bogoliubov-de Gennes (DBdG) quasiparticles of graphene. Josephson effect has also been studied in a superconductor-normal metal-superconducting (SNS) junction in graphene^{12,16}. It has been shown in Ref. 12, that the behavior of such junctions is similar to conventional SNS junctions with disordered normal region. Such Josephson junctions with thin barrier regions have also been experimentally realized recently¹⁷. However, Josephson effect in graphene superconductor-barrier-superconductor (SBS) junctions

has not been studied so far.

In this work, we study Josephson effect in graphene for tunnel SBS junctions. In this study, we shall concentrate on SBS junctions with barrier thickness d where λ is the superconducting coherence length, and width L which has an applied gate voltage V_0 across the barrier region. Our central result is that in complete contrast to the conventional Josephson tunnel junctions studied so far^{18,19}, the Josephson current in graphene SBS tunnel junctions is an oscillatory function of both the barrier thickness d and the applied gate voltage V_0 . We provide an analytical expression for the Josephson current of such a junction. We also compute the critical current of graphene SBS junctions. We find that this critical current is also an oscillatory function of V_0 and d and study the amplitude and periodicity of its oscillation. We also show that in the thin barrier limit, where the barrier region can be characterized by an effective dimensionless barrier strength $\gamma = V_0 d \sim v_F$ (v_F being the Fermi velocity of electrons in graphene), the Josephson current becomes an oscillatory function of γ with period π ¹⁴. We find that in this limit, the oscillatory behavior of Josephson current can be understood as a consequence of transmission resonance phenomenon of Dirac-Bogoliubov-de Gennes (DBdG) quasiparticles in graphene. We demonstrate that the Josephson current reaches the Kulik-Omyanchuk limit²⁰ for $\gamma = n$ (n being an integer), but, unlike conventional junctions, never reaches the Ambegaokar-Baratoff limit²¹ for large γ . We also discuss simple experiments to test our theory.

The organization of the rest of the paper is as follows. In Sec. II, we obtain an analytical expression for Josephson current for a general SBS junction of thickness d and applied voltage V_0 and demonstrate that the Josephson current is an oscillatory function of both d and V_0 . This is followed by Sec. III, where we discuss the limiting case of thin barrier and demonstrate that the oscillatory behavior of the Josephson current can be understood in terms of transmission resonance of DBdG quasiparticles in graphene. Finally we discuss experimental relevance of our results in Sec. IV.

II. JOSEPHSON CURRENT FOR TUNNEL SBS JUNCTIONS

We consider a SBS junction in a graphene sheet of width L lying in the xy plane with the superconducting regions extending $x = -1$ to $x = -d$ and from $x = 0$ to $x = 1$ for all $0 \leq y \leq L$, as shown in Fig 1. The superconducting regions $x = -1$ to $x = -d$ and $x = 0$ to $x = 1$ shall be assumed to be kept close to superconducting electrodes so that superconductivity is induced in these regions via proximity effect^{10,11}. Alternatively, one can also possibly use intercalated graphene which may have s -wave superconducting phases¹³. In the rest of this work, we shall assume that these regions are superconducting without worrying about the details of the mechanism used to induce superconductivity. The region B, modeled by a barrier potential V_0 , extends from $x = -d$ to $x = 0$. Such a local barrier can be implemented by either using the electric field effect or local chemical doping^{4,5}. In the rest of this work, we shall assume that the barrier region has sharp edges on both sides which requires $d = 2\pi k_F$, where k_F and π are the Fermi wave-vector and Fermi wavelength for graphene. Such barriers can be realistically created in experiments⁵. The width L of the sample shall be assumed to be large compared to all other length scales in the problem. The SBS junction can then be described by the DBdG equations¹⁰

$$\begin{pmatrix} H_a & E_F + U(x) \\ (x) & E_F - U(x) \end{pmatrix} \begin{pmatrix} \psi_a \\ \psi_b \end{pmatrix} = E_a \begin{pmatrix} \psi_a \\ \psi_b \end{pmatrix} \quad (1)$$

Here, $\psi_a = (\psi_{aK}; \psi_{aK^0}; \psi_{aA}; \psi_{aB})$ are the 4 component wavefunctions for the electron and hole spinors, the index a denote K or K^0 for electron/holes near K and K^0 points, a takes values $K^0(K)$ for $a = K(K^0)$, E_F denote the Fermi energy, A and B denote the two inequivalent sites in the hexagonal lattice of graphene, and the Hamiltonian H_a is given by

$$H_a = -i\psi_a (\sigma_x \partial_x + \text{sgn}(a) \sigma_y \partial_y); \quad (2)$$

where $\text{sgn}(a)$ takes values ± 1 for $a = K(K^0)$.

The pair-potentials $U(x)$ in Eq. 1 connects the electron and the hole spinors of opposite Dirac points. We have modeled the pair-potential as

$$U(x) = \Delta_0 [\exp(i\phi_2)(x) + \exp(i\phi_1)(x+d)]; \quad (3)$$

where Δ_0 is the amplitude and $\phi_{1(2)}$ are the phases of the induced superconducting order parameters in regions I (II) as shown in Fig. 1, and θ is the Heaviside step function. Notice that the mean-field conditions for superconductivity is satisfied as long as $\Delta_0 \neq 0$ or equivalently $k_F \neq 0$, where $\Delta_0 = \pi v_F$ is the superconducting coherence length¹². The potential $U(x)$ gives the relative shift of Fermi energies in the barrier and superconducting regions and is modeled as

$$U(x) = V_0 \theta(x) \theta(x+d); \quad (4)$$

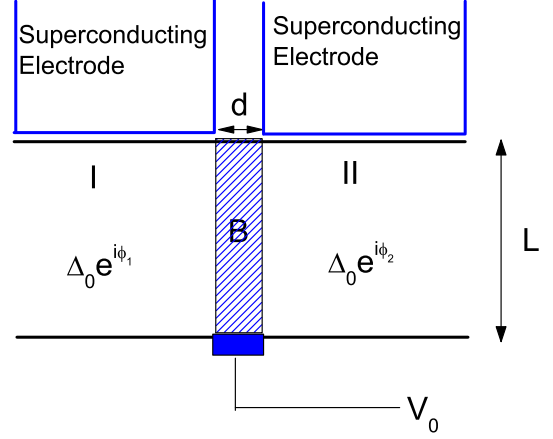


FIG. 1: A schematic graphene SBS junction with the barrier B sandwiched between two superconductors I and II with pair potentials $\Delta_0 e^{i\phi_1}$ and $\Delta_0 e^{i\phi_2}$. The barrier region is created by an external gate voltage V_0 .

Solving Eq. 1, we obtain the wavefunctions in the superconducting and the barrier regions. In region I, for the DBdG quasiparticles moving along x direction with a transverse momentum $k_y = q = 2\pi n/L$ (for integer n) and energy E , the wavefunctions are given by¹⁰

$$\psi_I = u_1; u_2; u_3; u_4 e^{i(k_s x + qy + \theta)}; \quad (5)$$

where

$$\begin{aligned} \frac{u_2}{u_1} &= \exp(-i\theta); \quad \frac{u_3}{u_1} = \exp[i(\theta_1 - \theta)]; \\ \frac{u_4}{u_1} &= \exp[i(\theta_1 + \theta)]; \end{aligned} \quad (6)$$

and $\int_{-1/4}^1 |u_i|^2 dx = 2$ is the normalization condition for the wavefunction for $d = 1$, where $\theta_1 = (\pi v_F)^2 k_s = E_F \sin(\theta)$ is the localization length. Here $k_s = (E_F - \pi v_F)^2 / \pi^2$, θ , the angle of incidence for the quasiparticles, is given by $\sin(\theta) = \pi v_F q / E_F$, and θ is given by

$$\begin{aligned} \theta &= \cos^{-1}(\theta_1 / E_F) \quad \text{if } |j| < \theta_1; \\ \theta &= i \cosh^{-1}(\theta_1 / E_F) \quad \text{if } |j| > \theta_1; \end{aligned} \quad (7)$$

Note that for $|j| > \theta_1$, θ becomes imaginary and the quasiparticles can propagate in the bulk of the superconductor. The wavefunctions in region II ($x > 0$) can also be obtained in a similar manner

$$\psi_{II} = v_1; v_2; v_3; v_4 e^{i(k_s x + qy + \theta)}; \quad (8)$$

where $\int_{-1/4}^1 |v_i|^2 dx = 2$ and the coefficients v_i are given

by

$$\begin{aligned}\frac{v_2}{v_1} &= \exp(-i\theta); \quad \frac{v_3}{v_1} = \exp[-i(\theta_2 + \theta)]; \\ \frac{v_4}{v_1} &= \exp[-i(\theta_1 + \theta)];\end{aligned}\quad (9)$$

The wavefunctions for electrons and holes moving along x in the barrier region is given by

$$\begin{aligned}\psi_B^e &= 1; e^{-i\theta}; 0; 0 \exp[i(k_b x + qy)] = \frac{p}{2d}; \\ \psi_B^h &= 0; 0; 1; e^{-i\theta} \exp[i(k_b^0 x + qy)] = \frac{p}{2d};\end{aligned}\quad (10)$$

Here the angle of incidence of the electron (hole) (θ) is given by

$$\begin{aligned}\sin[\theta] &= \frac{\sim v_F q}{s + (\theta)(E_F - V_0)} \\ k_b(k_b^0) &= \frac{+ (\theta)(E_F - V_0)^2}{\sim v_F} q^2\end{aligned}\quad (11)$$

To compute the Josephson current in the SBS junction, we now find the energy dispersion of the subgap Andreev bound states which are localized with localization length ~ 1 at the barrier^{22,23}. The energy dispersion ϵ_n (corresponding to the subgap state characterized by the quantum number n) of these states depends on the phase difference $\theta = \theta_2 - \theta_1$ between the superconductors. It is well known that the Josephson current I across the junction at a temperature T_0 is given by^{12,22}

$$I(\theta; T_0) = \frac{4eX}{\sim} \sum_{n, q=-k_F}^{k_F} \frac{\partial \epsilon_n}{\partial \theta} f(\epsilon_n); \quad (12)$$

where $f(x) = 1/(\exp(x/(k_B T_0)) + 1)$ is the Fermi distribution function and k_B is the Boltzmann constant²⁴.

To obtain these subgap Andreev bound states, we now impose the boundary conditions at the barrier. The wavefunctions in the superconducting and barrier regions can be constructed using Eqs. 5, 8 and 10 as

$$\begin{aligned}\psi_I &= a_1^+ \psi_I^+ + b_1^- \psi_I^-; \quad \psi_{II} = a_2^+ \psi_{II}^+ + b_2^- \psi_{II}^-; \\ \psi_B &= p \psi_B^e + q \psi_B^h + r \psi_B^{h+} + s \psi_B^{h-};\end{aligned}\quad (13)$$

where a_1 (a_2) and b_1 (b_2) are the amplitudes of right and left moving DBdG quasiparticles in region I(II) and p (q) and r (s) are the amplitudes of right (left) moving electron and holes respectively in the barrier. These wavefunctions must satisfy the boundary conditions:

$$\psi_I|_{x=d} = \psi_B|_{x=d}; \quad \psi_B|_{x=0} = \psi_{II}|_{x=0}; \quad (14)$$

Notice that these boundary conditions, in contrast their counterparts in standard SBS interfaces²³, do not impose any constraint on derivative of the wavefunctions. Thus

the standard delta function potential approximation for short barriers^{22,23} can not be taken the outset, but has to be taken at the end of the calculations.

Substituting Eqs. 5, 8, 10, and 13 in Eq. 14, we find the equations for boundary conditions at $x = d$ to be

$$\begin{aligned}a_1 e^{ik_b d} + b_1 e^{ik_b^0 d} &= p e^{ik_b d} + q e^{ik_b^0 d} \\ a_1 e^{i(\theta_1 + k_b d)} + b_1 e^{i(\theta_1 + k_b^0 d)} &= r e^{i(\theta_1 + k_b d)} + s e^{i(\theta_1 + k_b^0 d)} \\ a_1 e^{i(\theta_1 + k_b d)} + b_1 e^{i(\theta_1 + k_b^0 d)} &= r e^{i(\theta_1 + k_b d)} + s e^{i(\theta_1 + k_b^0 d)}\end{aligned}\quad (15)$$

Similar equations at $x = 0$ reads

$$\begin{aligned}a_2 + b_2 &= p + q \\ a_2 e^{i(\theta_2 + k_b d)} + b_2 e^{i(\theta_2 + k_b^0 d)} &= r + s \\ a_2 e^{i(\theta_2 + k_b d)} + b_2 e^{i(\theta_2 + k_b^0 d)} &= r e^{i\theta} + s e^{i\theta}\end{aligned}\quad (16)$$

Eqs. 15 and 16 therefore yields eight linear homogeneous equations for the coefficients $a_{i=1,2}$, $b_{i=1,2}$, p , q , r , and s , so that the condition for non-zero solutions of these coefficients can be obtained as

$$A^0 \sin(2\theta) + B^0 \cos(2\theta) + C^0 = 0 \quad (17)$$

where A^0 , B^0 , and C^0 are given by

$$\begin{aligned}A^0 &= \cos(k_b^0 d) \cos(\theta) \cos(\theta) \sin(k_b d) (\sin(\theta) \sin(\theta) - 1) \\ &\quad + \cos(k_b d) \cos(\theta) \cos(\theta) \sin(k_b^0 d) \\ &\quad + \frac{1}{2} \cos(k_b d) \cos(\theta) \sin(2\theta) \sin(\theta) \sin(k_b^0 d) \\ B^0 &= \sin(k_b^0 d) \sin(k_b d) (1 + \sin(\theta) \sin(\theta) \\ &\quad + \sin(\theta) \sin(\theta) \sin^2(\theta)) \\ &\quad + \cos(k_b d) \cos(k_b^0 d) \cos^2(\theta) \cos(\theta) \cos(\theta) \\ C^0 &= \cos^2(\theta) \cos(\theta) \cos(\theta) \cos(\theta) - \sin(k_b d) \sin(k_b^0 d) \\ &\quad + \sin(\theta) \sin(\theta) \sin^2(\theta) \\ &\quad + \sin(\theta) (\sin(\theta) - \sin(\theta))\end{aligned}\quad (18)$$

Note that in general the coefficients A^0 , B^0 , and C^0 depends on θ through k_b , k_b^0 , and θ which makes it impossible to find an analytical solution for Eq. 17. However, for subgap states in graphene SBS junctions, $\theta \approx E_F$. Further, for short tunnel barrier we have $j_0 \approx E_F$. In this regime, as can be seen from Eqs. 11, A^0 , B^0 , and C^0 become independent of θ since $k_b \approx k_b^0 \approx k_1 = \frac{[(E_F - V_0) - \sim v_F]^2}{2}$ and $\theta \approx \theta_1 = \sin^{-1}[\sim v_F q / (E_F - V_0)]$ so that the dependence of k_b , k_b^0 , and θ can be neglected. In this regime one finds that $A^0, B^0, C^0 \neq 0$; $A/B, B/C$ where

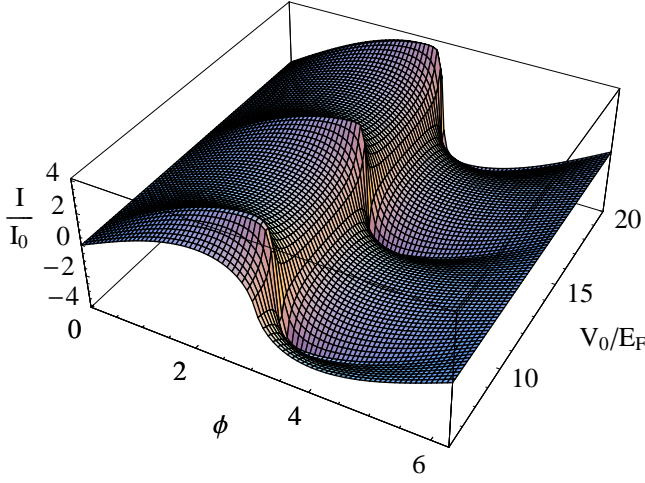


FIG. 2: Plot of Josephson current I as a function of phase difference ϕ and the applied gate voltage V_0 for $k_B T_0 = 0.01$ eV and $d = 0.5$ nm showing oscillatory behavior of I/I_0 as a function of the applied gate voltage.

$$\begin{aligned}
 A &= 0 \\
 B &= \sin^2(k_1 d) [1 - \sin(\phi) \sin(\phi_1)]^2 \\
 &\quad \cos^2(k_1 d) \cos^2(\phi) \cos^2(\phi_1) \\
 C &= \sin^2(k_1 d) [\sin(\phi) - \sin(\phi_1)]^2 \\
 &\quad + \cos^2(\phi) \cos^2(\phi_1) \cos(\phi)
 \end{aligned} \quad (19)$$

The dispersion of the Andreev subgap states can now be obtained from Eqs. 17 and 7. One finds that there are two Andreev subgap states with energies $E_{\pm} = \pm \sqrt{B^2 - C}$ where

$$B = \sum_{n=0}^{\infty} \frac{(-1)^n}{n!} \frac{C^n}{C=2B} \quad (20)$$

Using Eq. 12, one can now obtain the expression for the Josephson current

$$\begin{aligned}
 I(\phi; V_0; d; T_0) &= I_0 g(\phi; V_0; d; T_0); \\
 g(\phi; V_0; d; T_0) &= \frac{2}{\pi} \int_0^{\pi} d\theta \frac{\cos^3(\theta) \cos^2(\phi_1) \sin(\theta)}{\sqrt{B^2 - C}} \\
 &\quad \tanh\left(\frac{2k_B T_0}{\hbar v_F}\right)
 \end{aligned} \quad (21)$$

where $I_0 = \frac{e}{\hbar} \frac{2\pi}{L} \frac{\hbar^2}{2m} \frac{1}{v_F} \frac{1}{2} \frac{1}{d} \cos(\phi)$ and we have replaced $\frac{1}{L} \frac{1}{d} \cos(\phi)$ as appropriate for wide junctions¹².

Eqs. 20, and 21 represent the central result of this work. From these equations, we find that both the dispersion of the Andreev subgap states and the Josephson current in graphene SBS junctions, in complete contrast to their conventional counterparts^{18,19,22}, is oscillatory function of the applied gate voltage V_0 and the barrier thickness d . This statement can be most easily

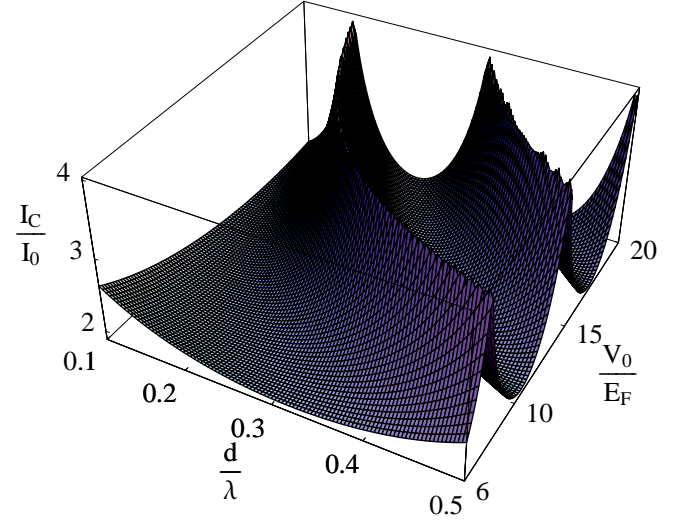


FIG. 3: Plot of I_c/I_0 vs the applied gate voltage V_0 and the junction thickness d for $T_0 = 0.01$ eV.

checked by plotting the Josephson current I as a function of the phase difference ϕ and the applied gate voltage V_0 for a representative barrier thickness $d = 0.5$ nm and temperature $k_B T_0 = 0.01$ eV, as done in Fig. 2. In Fig. 3, we plot the critical current of these junctions $I_c(V_0; d; T_0) = \max_{\phi} [I(\phi; V_0; d; T_0)]$ as a function of the applied gate voltage V_0 and barrier thickness d for low temperature $k_B T_0 = 0.01$ eV. We find that the critical current of these graphene SBS junctions is an oscillatory function of both V_0 and d . This behavior is to be contrasted with those of conventional junctions where the critical current is a monotonically decreasing function of both applied bias voltage V_0 and junction thickness d ^{18,19,22}.

Next, we analyze the temperature dependence of the amplitude of oscillations of I_c . To find the amplitude of oscillation, we have computed I_c as a function of V_0 (for a representative value of $d = 0.3$ nm), noted the maximum (I_c^{\max}) and minimum (I_c^{\min}) values of I_c , and calculated the amplitude $I_c^{\max} - I_c^{\min}$. The procedure is repeated for several temperatures T_0 and the result is plotted in Fig. 4 which shows that the amplitude of oscillations decreases monotonically as a function of temperature.

Finally, we discuss the period of oscillation of the critical current. To obtain the period, we obtain the critical current I_c as a function of barrier width d for the fixed applied gate voltage V_0 and note down d_{period} . We then compute $\text{period} = V_0 d_{\text{period}} \approx \hbar v_F$ and plot period as a function of V_0 for $k_B T_0 = 0.01$ eV as shown in Fig. 5. We find that period decreases with V_0 and approaches an universal value for large $V_0 \gg 20 E_F$. This property, as we shall see in the next section, can be understood by analysis of graphene SBS junctions in the thin barrier limit ($V_0 \gg 1$ and $d \rightarrow 0$ such that $V_0 d \approx \hbar v_F$ remains finite¹⁴) and is a direct consequence of transmiss-

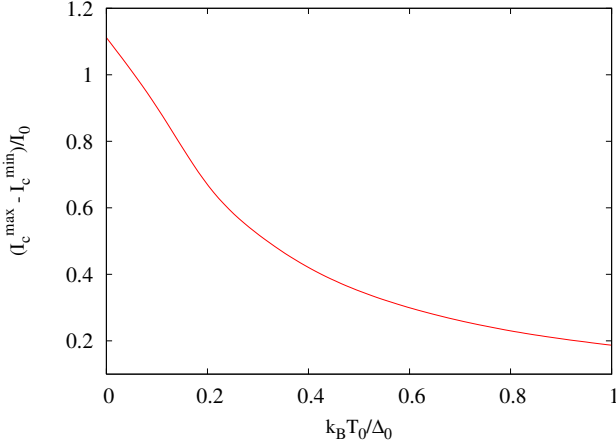


FIG. 4: Plot of the temperature dependence of the amplitude of oscillations of I_c (given by $[I_c^{\max}(d) - I_c^{\min}(d)]/I_0$) for $d = 0.3$. The amplitude is measured by noting the maximum and minimum values of the critical current by varying V_0 for a fixed d .

sion resonance phenomenon of DBdG quasiparticles in superconducting graphene.

III. THIN BARRIER LIMIT

In the limit of thin barrier, where $V_0 \gg 1$ and $d \ll 0$ such that $\epsilon = V_0 d \sim v_F$ remains finite, $\epsilon_1 \ll 0$ and $k_1 d \ll 1$. From Eqs. 19 and 20, we find that in this limit, the dispersion of the Andreev bound states becomes

$$I^{\text{tb}}(q; \epsilon; T) = \frac{q}{0.1} \frac{T(\epsilon; T) \sin^2(\epsilon/2)}{\cos^2(\epsilon/2)}; \quad (22)$$

$$T(\epsilon; T) = \frac{\cos^2(\epsilon/2)}{1 - \cos^2(\epsilon/2) \sin^2(\epsilon/2)}; \quad (23)$$

where the superscript 'tb' denote thin barrier limit. The Josephson current I can be obtained substituting Eq. 23 in Eq. 12. In the limit of wide junctions, one gets

$$I^{\text{tb}}(\epsilon; T_0) = I_0 g^{\text{tb}}(\epsilon; T_0);$$

$$g^{\text{tb}}(\epsilon; T_0) = \frac{1}{d} \sum_{n=-\infty}^{\infty} \frac{T(\epsilon; T_0) \cos(\epsilon/2) \sin(\epsilon/2)}{1 - T(\epsilon; T_0) \sin^2(\epsilon/2)} \tanh(\epsilon/2k_B T_0); \quad (24)$$

Eqs. 23, and 24 represent the key results of this section. From these equations, we find that the Josephson current in graphene SBS junctions is a periodic oscillatory function of the effective barrier strength in the thin barrier limit. Further we observe that the transmission probability of the DBdG quasiparticles in a thin SBS junction is given by $T(\epsilon; T)$ which is also the transmission probability of a Dirac quasiparticle

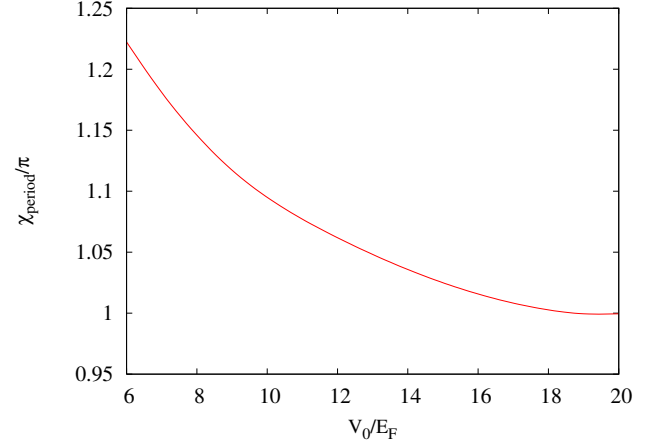


FIG. 5: Plot of χ_{period} of the critical current I_c as a function of V_0 . Note that χ_{period} approaches 1 as we approach the thin barrier limit.

through a square potential barrier as noted in Ref. 5. Note that the transmission becomes unity for normal incidence ($\epsilon = 0$) and when $\epsilon = n\pi$. The former condition is a manifestation of the Klein paradox for DBdG quasiparticles⁵. However, this property is not reflected in the Josephson current which receives contribution from quasiparticles approaching the junction at all angles of incidence. The latter condition ($\epsilon = n\pi$) represents transmission resonance condition of the DBdG quasiparticles. Thus the barrier becomes completely transparent to the approaching quasiparticles when $\epsilon = n\pi$ and in this limit the Josephson current reduces to its value for conventional tunnel junctions in the Kulik-Omel'yanchuk limit: $I^{\text{tb}}(\epsilon; n; T_0) = 4I_0 \sin(\epsilon/2) \text{Sgn}(\cos(\epsilon/2)) \tanh(\epsilon/2k_B T_0)$ ²⁰. This yields the critical Josephson current $I_c^{\text{tb}}(\epsilon = n\pi) = 4I_0$ for $k_B T_0 \ll \epsilon$. Note, however, that in contrast to conventional junctions $T(\epsilon; T)$ can not be made arbitrarily small for all ϵ by increasing T . Hence I_c^{tb} never reaches the Ambegaokar-Baratoff limit of conventional tunnel junctions²¹. Instead, $I_c^{\text{tb}}(\epsilon)$ becomes a periodic oscillatory function of ϵ . The amplitude of these oscillations decreases monotonically with temperature as discussed in Sec. II.

Finally, we compute the product $I_c^{\text{tb}} R_N$ which is routinely used to characterize Josephson junctions^{18,19}, where R_N is the normal state resistance of the junction. For graphene SBS junctions R_N corresponds to the resistance of a Dirac quasiparticle as it moves across a normal metal barrier-normal metal junction. For short and wide junctions discussed here, it is given by $R_N = R_0 s_1(\epsilon)$ where $R_0 = \frac{2}{v_F} \sim \frac{2}{e^2 E_F L}$ and $s_1(\epsilon)$ is given by^{5,12}

$$s_1(\epsilon) = \frac{1}{d} \sum_{n=-\infty}^{\infty} T(\epsilon; T) \cos(\epsilon/2); \quad (25)$$

Note that $s_1(\epsilon)$ and hence R_N is an oscillatory function of ϵ with minimum $0.5R_0$ at $\epsilon = n\pi$ and maximum

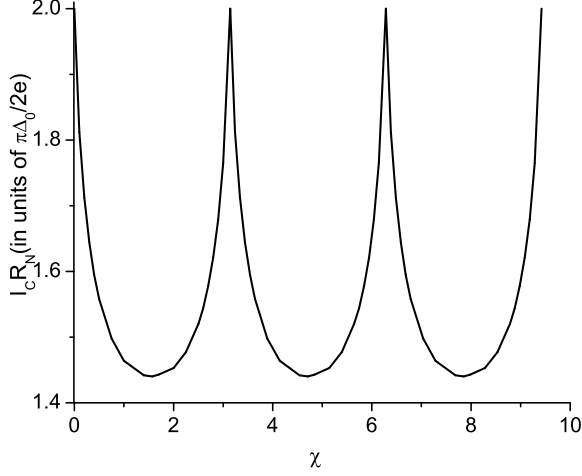


FIG. 6: Plot of $I_c^{\text{tb}} R_N$ as a function of χ . $I_c^{\text{tb}} R_N$ is an oscillatory bounded function of χ and never reaches its value ($\phi_0 = 2e$) for conventional junctions in the Ambegaokar-Barato limit.

$0.75R_0$ at $\chi = (n + 1/2)$. The product $I_c^{\text{tb}} R_N$, for thin SBS junctions is given by

$$I_c^{\text{tb}} R_N = (\phi_0 = 2e) g_{\text{max}}^{\text{tb}}(\chi; T) = s_1(\chi); \quad (26)$$

where $g_{\text{max}}^{\text{tb}}(\chi)$ is the maximum value of $g^{\text{tb}}(\chi; T)$. Note that $I_c^{\text{tb}} R_N$ is independent of E_F and hence survives in the limit $E_F \rightarrow 0$ ¹². For $k_B T_0 \rightarrow 0$, $g_{\text{max}}^{\text{tb}}(\chi) = 4$ and $s_1(\chi) = 2$, so that $I_c^{\text{tb}} R_N|_{\chi=n} = \phi_0 = 2e$ which coincides with Kulik-Omel'yanchuk limit for conventional tunnel junctions^{20,23}. However, in contrast to the conventional junction, $I_c^{\text{tb}} R_N$ for graphene SBS junctions do not monotonically decrease to the Ambegaokar-Barato limit^{21,23} of $\phi_0 = 2e \approx 1.57 \phi_0 = e$ as χ is increased, but

demonstrates periodic oscillatory behavior and remains bounded between the values $\phi_0 = e$ at $\chi = n$ and $2.27 \phi_0 = e$ at $\chi = (n + 1/2)$, as shown in Fig. 6.

IV. EXPERIMENTS

As a test of our predictions, we suggest measuring DC Josephson current in these junctions as a function of the applied voltage V_0 . Such experiments for conventional Josephson junctions are well-known²⁵. Further SNS junctions in graphene has also been recently been experimentally created¹⁷. For experiments with graphene junctions which we suggest, the local barrier can be fabricated by applying an additional gate voltage in the normal region of the junctions studied in Ref. 17. In graphene, typical Fermi energy can reach $E_F \approx 80 \text{ meV}$ with Fermi wavelength $\lambda_F = 2\pi/k_F \approx 100 \text{ nm}$ ⁵. Effective barrier strengths of $500 - 1000 \text{ meV}$ and barrier widths of $d \approx 20 - 50 \text{ nm}$ can be achieved in realistic experiments^{4,5}. These junctions therefore meet our theoretical criteria: $d \ll \lambda_F$ and $j_0 \gg E_F$. To observe the oscillatory behavior of the Josephson current, it would be necessary to change V_0 in small steps ΔV_0 . For barriers with fixed $d = 0.3$ and $V_0 = E_F = 10$, this would require changing V_0 in steps of approximately 30 meV which is experimentally feasible. The Joule heating in such junctions, proportional to $I_c^2 R_N$, should also show measurable oscillatory behavior as a function of V_0 .

In conclusion, we have shown that the Josephson current in graphene SBS junction shows novel oscillatory behavior as a function of the applied bias voltage V_0 and the barrier thickness d . In the thin barrier limit, such a behavior is the manifestation of transmission resonance of DBdG quasiparticles in superconducting graphene. We have suggested experiments to test our predictions.

KS thanks V.M. Yakovenko for discussions.

¹ K.S. Novoselov et al. Science 306, 666 (2004).

² T. Ando, J. Phys. Soc. Jpn. 74 777 (2005).

³ V.P. Gusynin and S.G. Sharapov, Phys. Rev. Lett. 95, 146801 (2005); N.M.R. Peres, F. Guinea, and A. Castro Neto, Phys. Rev. B 73, 125411 (2006).

⁴ K.S. Novoselov et al. Nature 438, 197 (2005); Y. Zhang et al. Nature 438, 201 (2005).

⁵ M.J. Katsnelson et al. Nature Phys. 2, 620 (2006).

⁶ O. Klein, Z. Phys. 53, 157 (1929).

⁷ V. Lukose, R. Shankar and G. Baskaran, Phys. Rev. Lett., 98 116802 (2007).

⁸ K. Sengupta and G. Baskaran, arXiv:0705.0257 (unpublished).

⁹ M. Hentschel and F. Guinea, arXiv:0705.0522 (unpublished).

¹⁰ C.W.J. Beenakker, Phys. Rev. Lett. 97, 067007 (2006).

¹¹ A.F. Volkov et al., Physica C 242, 261 (1995).

¹² M. Titov and C.W.J. Beenakker, Phys. Rev. B 74,

041401(R) (2006).

¹³ B.Uchoa and A. Castro Neto, Phys. Rev. Lett. 98, 146801 (2007).

¹⁴ S. Bhattacharjee and K. Sengupta, Phys. Rev. Lett. 97, 217001 (2006).

¹⁵ S. Bhattacharjee, M. Maiti and K. Sengupta, arXiv:0704.2760 (unpublished).

¹⁶ A.G. Moghaddam and M. Zareyan, cond-mat/0611577 (unpublished).

¹⁷ H. Heersche et al., Nature 446, 56 (2006).

¹⁸ K.K. Likharev, Rev. Mod. Phys. 51, 101 (1979).

¹⁹ A.A. Golubov, M.Y. Kupriyanov, and E. Il'ichev, Rev. Mod. Phys. 76, 411 (2004).

²⁰ I.O. Kulik and A.Omel'yanchuk, JETP Lett. 21, 96 (1975); ibid Sov. Phys. JETP 41, 1071 (1975).

²¹ V. Ambegaokar and S. Barato, Phys. Rev. Lett. 10, 486, (1963).

²² A.M. Zagorskii Quantum Theory of Many Body Systems,

Springer-Verlag, New York (1998).

- ²³ H.-J. Kown, K. Sengupta and V. M. Yakovenko, Eur. Phys. J. B 37, 349 (2004).
- ²⁴ For short junctions ($d \ll \lambda_F$), the main contribution to the Josephson current comes from the subgap states¹².
- ²⁵ P. W. Anderson and J. Rowel, Phys. Rev. Lett. 10, 230 (1963).